

# Evaluation of UHPFRC activation energy using empirical models

A. Kamen · E. Denarié · H. Sadouki · E. Brühwiler

Received: 5 September 2007 / Accepted: 27 June 2008 / Published online: 8 July 2008  
© RILEM 2008

**Abstract** The influence of thermal curing on the evolution of the material properties and the UHPFRC behaviour was investigated. Tests results showed a beneficial effect of a high temperature curing on the early age material properties due to the thermo-activation effect on the hydration process. However, an inverse effect was observed at long-term. In our study, activation energy of UHPFRC was evaluated from experimental data by means of empirical models. The traditional maturity-function based on Arrhenius law, generally used to describe thermally activated physical or chemical processes, was used to predict the evolution of the UHPFRC autogenous shrinkage and to validate the applicability of this concept for such cement-based materials. Results showed that the concept based on Arrhenius law could describe correctly temperature effects on UHPFRC for temperature lower than 30°C.

**Résumé** L'influence de la cure thermique sur l'évolution des propriétés et du comportement du Béton Fibré Ultra Performant (BFUP) a été étudiée. Les résultats d'essais ont montré l'effet bénéfique des températures élevées sur les propriétés du matériau au jeune âge à cause de la thermo-activation du

*processus d'hydratation. Néanmoins, un effet inverse a été observé à long terme. Dans cette étude, l'énergie d'activation du BFUP a été évaluée à partir des résultats expérimentaux par le biais de modèles empiriques. Le concept de maturité traditionnel basé sur la loi d'Arrhenius, généralement utilisé pour décrire l'activation thermique des processus physiques et chimiques, a été utilisé pour prédire l'évolution du retrait endogène du BFUP et pour valider l'application de ce concept pour de tels matériaux cimentaires. Les résultats ont montré que le concept basé sur la loi d'Arrhenius décrit correctement l'effet thermique sur le BFUP pour des températures inférieures à 30°C.*

**Keywords** UHPFRC · Temperature effect · Activation energy · Autogenous shrinkage

## 1 Introduction

Usually, the material properties (mechanical and chemical) are determined with respect to the norms and at reference temperature i.e. 20°C. In this research, the idea was to measure the fundamental properties of UHPFRC cured at different curing temperature in the aim to show that the curing conditions could induce an artefact: initial (thermal) stress which would have an impact on certain properties. This work is a part of the first author

A. Kamen (✉) · E. Denarié · H. Sadouki · E. Brühwiler  
Laboratory of Maintenance and Safety of Structures  
(MCS), Ecole Polytechnique Fédérale de Lausanne  
(EPFL), Station 18, Lausanne 1015, Switzerland  
e-mail: aicha.kamen@epfl.ch

PhD thesis untitled “behavior at early age of UHPFRC under thermo-mechanical effects” [1].

It is known, that the early age behavior is complex and several processes interact simultaneously and are influenced by the environment conditions. During the PhD research an extensive experimental study was carried out (1) to study the effect of curing conditions on the fundamental properties of the UHPFRC, particularly the autogenous shrinkage that is the main source of early age cracks in specific structures (under particular structural and environmental conditions) due to the high induced tensile stresses. Early age cracks potentially compromise the durability of newly constructed or repaired structures. (2) to understand the correlation between the phenomenon’s and (3) to highlight some new points which were not considered in previous research on such an innovative material. Besides, the aim of the PhD research was to model the fundamental properties for arbitrary temperature history. These models are necessary to predict accurately the deformations, the stresses and the damage (cracking) in the case of structural elements subjected to in-situ temperature variations. And finally, to predict the behavior of engineer elements structures using finite element software MLS (Multi Layer System) based on a series of models and accounting for their interactions. In this software the maturity concept is used to describe certain material properties. Such numerical simulations that can be performed before the conception may be beneficial in reducing the early age cracking risk thanks to a better understanding of the curing conditions influence considered as most influential early age factor.

In the past, the maturity function was introduced to account for the combined effects of time and temperature on the concrete strength evolution. According to Saul 51 “*Concrete of the same mix at the same maturity has approximately the same strength whatever combination of temperature and time go to make up that maturity*” [2]. It was confirmed later by the National Bureau of Standards (NBS) that the maturity method could be used to estimate the development of mechanical properties of concrete [2]. In 1977, a new function based on the Arrhenius equation to calculate the equivalent age of concrete was proposed by Hansen and Pedersen [3].

The maturity concept could describe the materials properties dependant of hydration: heat of hydration,

the chemical shrinkage, and the autogenous deformations [4]. Other recent research works showed that the usual maturity concept is not valid for the autogenous deformation which is strongly influenced by the temperature history [5, 6].

On the other hand [7], showed that the maturity concept is applicable for the prediction of the autogenous shrinkage of cement pastes for temperatures between 10 and 40°C, while it does not apply for higher temperatures. To overcome this problem the authors suggested to use various activation energies. This proposition was validated by Mounouga [8].

This paper focuses on the influence of curing temperature on certain UHPFRC properties, namely: hydration, self desiccation, deformations and mechanical properties and on the validation of maturity concept for this specific material.

## 2 Material and test program

### 2.1 Material

The experimental tests were carried out on Ultra High Performance Fibre Reinforced Concrete of the CEMTEC<sup>®</sup><sub>multiscale</sub> family [9]. The specific UHPFRC can be used in composite concrete structural members, as overlays on existing or new structures to locally “harden” the critical zones subjected to an aggressive environment and to significant mechanical stresses. It can be used also for specific thin structural members as crash barrier to limit the heat release during the hydration of binder (high amount of cement and silica fume as shown in Table 3). For instance, the real evolution of temperature in the core of the UHPFRC layer of composite beams (UHPFRC-NC) investigated by Habel [10] showed an increase from 20 to 32°C due to hydration process. Our research focuses on the behaviour of this material when it is used as overlays on existing structural elements exposed to aggressive environment.

The tested UHPFRC is produced by adding to ultra-compact cementitious matrix micro-fibres. They have a semi-circular section, with variable dimensions and present an irregular aspect ratio allowing a high adhesion with cementitious matrix. And straight steel fibres, with 10 mm length and 0.2 mm diameter and aspect ratio of 50. The total percentage of fibres being 9%



The matrix is composed of: (1) cement with low content of C<sub>3</sub>A, thus minimizing its water demand, (2) silica fume by product of zirconium production in high amount (26% by weight of cement), (3) fine quartz sand with 0.5 mm maximum grain size, (4) water and (5) high percentage (3.3% total by weight of cement) of superplasticizer in liquid form with solid content of approx 30%. The water content in the percentage is included in the water to cement ratio (W/C).

The Chemical compositions of the cement and silica fume are presented in Table 1, and mineralogical composition of the cement, determined by Bogue equations, is reported in Table 2. And finally the mix proportions of the tested UHPFRC are given in Table 3.

The properties of the present UHPFRC in fresh state and mean mechanical properties (compressive strength and modulus of elasticity on 11/22 cm cylinders,

**Table 1** Chemical compositions of CEM I 52.5 N CE PM-ES-CP2 NF Le Teil Produced by Lafarge and the silica fume SEPR

Component	Cement (%)	Silica fume (%)
SiO <sub>2</sub>	22.75	93.5
Al <sub>2</sub> O <sub>3</sub>	2.70	3.5
Fe <sub>2</sub> O <sub>3</sub>	1.90	0.15
CaO	67.10	0.02
MgO	0.75	–
K <sub>2</sub> O	0.20	0.06
Na <sub>2</sub> O	0.15	0.10
SO <sub>3</sub>	2.10	60 ppm
Insolubles	0.30	–
ZrO <sub>2</sub>	–	2.4
CO <sub>2</sub>	1.30	–
CaO free	0.55	–
LOI	1.90	0.5

**Table 2** Mineralogical composition according to Bogue

Phase	(%)
C3S	73.4
C2S	9.9
C3A	3.9
C4AF	5.8
	93.0
Others	7.02

**Table 3** UHPFRC recipe

Material	kg/m <sup>3</sup>
Cement (CEM I 52.5)/silica fume/fine sand	1410.2/367.0/80.4
Water/superplasticizer (chrysofluid optima 175)	200.1/46.5
Steel fibres (macro and micro)	706.5

**Table 4** Properties of fresh and hardened UHPFRC

Water/cement	0.165
Water/binder	0.131
Slump flow	65 cm
Air content	1.8%
Compressive strength at 7 days	163 MPa
E-Modulus at 7 days	43 GPa
Tensile strength at 7 days	15 MPa
Magnitude of tensile hardening strain	0.20%

uniaxial tensile strength and magnitude of tensile hardening on unnotched dogbone specimens of 70 cm long and 10 × 5 cm<sup>2</sup> cross section) at reference temperature 20°C are presented in Table 4.

## 2.2 Test program

Compressive strength was measured on three (4 × 4 × 16 cm<sup>3</sup>) prismatic specimens for each age (3, 7, 14 and 28 days). The specimens were cured at different temperatures (20, 30 and 40°C). The curing temperatures (30 and 40°C) were imposed a few minutes after casting the UHPFRC. The forms were sealed in plastic foil and placed in the oven. After removing the forms, the same procedure of sealing employed for the specimens cured at 20°C, was applied to the specimens cured at 30 and 40°C [1].

The degree of hydration of UHPFRC-matrix samples (without fibres) subjected to the same range of temperature was determined by the fire loss on ignition test at different ages (2, 3, 7, 14, 28 days) [11]. In this technique (LOI), the degree of hydration is calculated from the quantity of bound water (nonevaporable water). LOI constitutes an indirect degree of hydration measurement by supposing a linear relationship between the amount of bound water and the degree of hydration.

For those measurements, each sample was crushed in crushing-mill and finally ground. The material was then sieved on a 125  $\mu\text{m}$  sieve. The obtained powder was sealed in small plastic bags before being transported and weighed. Two samples of 50 g of powder were used for each measurement. Samples to be analyzed were placed in crucibles, and were introduced into a 105°C oven for 24 h (until constant weight was reached). At this temperature, it is assumed that all free water has evaporated. The samples were then weighed while the oven was heated to a temperature of 1,000°C. During the weighing process, the samples were kept in a desiccator with silica-gel to prevent the reabsorption of humidity. The samples were then again placed in a 1,000°C oven for 1 h, and weighed again. The quantity of bound water at time  $t$   $W_{ne}(t)$  can then be estimated through the mass loss between the 105°C and 1,000°C heating periods.

Self desiccation measurements were conducted at 7 days on cylinders for all temperatures using an embedded thermohygral probe [10]. This was done by placing UHPFRC matrix in a (3 × 5 cm) steel mould sealed with aluminium and plastic foils to minimize the exchange of humidity with the environment, Fig. 1a.

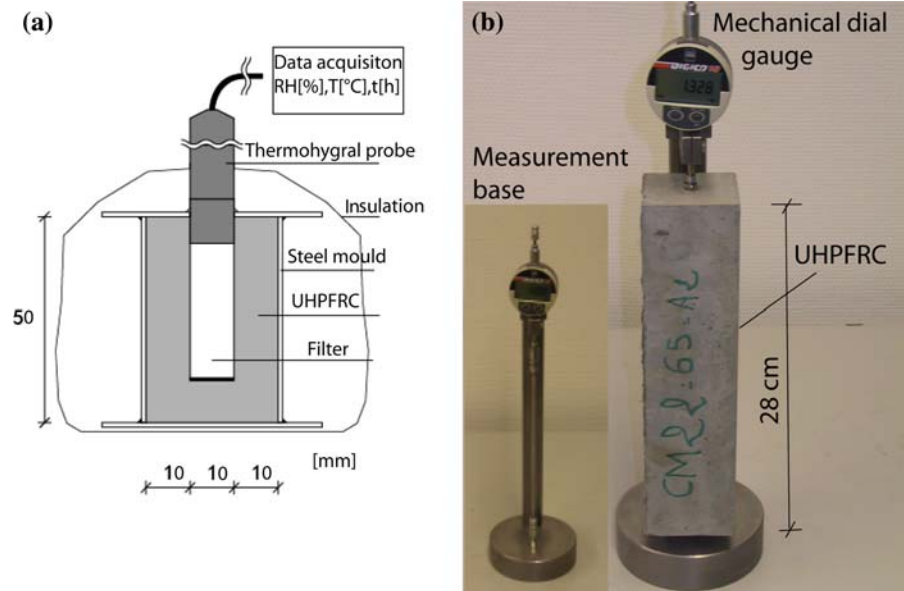
The autogenous shrinkage tests were performed on 7 × 7 × 28 cm<sup>3</sup> sealed prisms and starting at an age of 1.5 days. For this series of tests the authors used a standard device (retractometer) previously used to

measure linear autogenous shrinkage. In this measurement procedure the specimen must be removed from a mould and sufficiently hard before measurements starting. This UHPFRC is sufficiently hard at a curing time of 36 h (corresponding to the setting time for the current UHPFRC) due to high amount of superplasticizer. In other tests not included in this paper, the early age autogenous shrinkage was also investigated using a thermal stress testing machine (TSTM), which measures the early age linear deformation, starting 1 h after casting the material. Additional details concerning UHPFRC early age autogenous shrinkage measurement and results can be found in reference [1, 12].

Sealed conditions were implemented immediately after removing the forms, by applying double layers of self adhesive aluminium foil to prevent exchange with the external environment. The measurements were performed in climatically controlled room with temperature of  $20 \pm 1.25^\circ\text{C}$  and RH of 65%. For temperature (30 and 40°C), three specimens were removed from the oven and the measurements were performed within a short period of time in the same climatically controlled room. It is assumed that during this short time period there is no significant influence. After that the specimens were placed immediately again in the oven [13].

The measurements were conducted by means of a retractometer equipped with Tesa comparator,

**Fig. 1** (a) Self desiccation measurement set up, (b) autogenous shrinkage measurement set up



providing a measurement accuracy of about  $\pm 5\mu\text{m/m}$ . The set up is shown in Fig. 1b.

### 3 Effect of temperature on hydration and self-desiccation

The development of the degree of hydration and the relative humidity under different curing conditions are represented in Fig. 2. As expected, the development of the degree of hydration is accelerated at early age by increasing curing temperatures. For example, at  $40^\circ\text{C}$ , the degree of hydration at 2 days is 96% of its value at 28 days. Figure 2a shows that the degree of hydration curve at  $40^\circ\text{C}$  maintained right until 28 days. This is due to the consumption of all the available water ( $W/B = 0.131$ ). For  $30^\circ\text{C}$  curing, the degree of hydration reduces slightly, it is theorized that such a reduction in hydration can be attributed to variability in measurement over time. This can be seen also for standard tests as compressive tests or others, because the measurements are individual and not continuous in time. Note, the result showed here corresponds to the mean value of two specimens

An inverse effect of temperature on the degree of hydration is observed later and higher ultimate degree of hydration is obtained at  $20^\circ\text{C}$ . This transition occurred at approximately 7 days. This inverse relationship was explained according to [14] by a non-uniform distribution of hydration products with a high concentration around hydrating grains, thus retarding the hydration process under high curing, while at low temperature, diffusion and precipitation of the hydration products are relatively uniform.

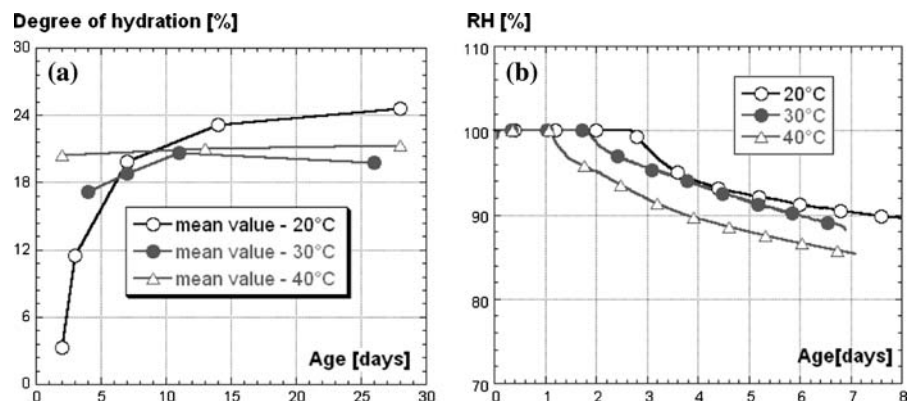
Moreover, according to the literature, high temperatures influence the stability and the structure of the hydration products especially the calcium silicate hydrates (C–S–H) and the rearrangement of the hydrates [14–16]. On the other hand, high temperatures favour the formation of the inner (C–S–H) and the modification of chains.

The self desiccation measurement corresponds to the moisture level within the concrete pores. When the voids are saturated the measured relative humidity is equal to 100%. This value diminishes during the hydration process as water is consumed and the gas volume within the concrete increases. Figure 2b shows that self-desiccation accelerates at higher temperatures. This result was expected as the equilibrium between the liquid and vapour phases depends on temperature [4, 17]. The ages of initiation of self-desiccation for the different curing conditions of temperatures curves are 2.7, 1.9, and 1.1 days respectively at 20, 30 and  $40^\circ\text{C}$ , and the relative humidity drops off to reach respectively 90.3, 88.2 and 85.5% at 7 days. This behaviour was attributed to the thermo-activation of the hydration process at early age and the resulting modification of the pore structure, which is traduced by a decrease of mean pore size and an increase of capillary depression, as showed by the calculated results according the Kelvin law under different curing conditions [17].

### 4 Effect of temperature on autogenous shrinkage

Autogenous shrinkage is negligible for normal concrete, but for cementitious materials with very low

**Fig. 2** (a) Evolution of the degree of hydration for different curing conditions, (b) evolution of the relative humidity for different curing conditions





$W/C$  ratios, becomes the dominant shrinkage mechanism.

The autogenous shrinkage curve at 20°C (Fig. 3), shows that the current UHPFRC exhibits moderate autogenous shrinkage, despite the high paste volume (88%) and the very low  $W/B$  (0.131). Its autogenous shrinkage is comparable to that measured in a high performance concrete with 0.2  $W/B$  ratio and 10% silica fume or self compacting concrete [1].

As the autogenous shrinkage is directly related to the hydration process. This moderate value of the autogenous shrinkage can be attributed in prior to the low degree of hydration (26% at 90 days) which is a primary characteristic of the material and to the high amount of fibres (9% by volume) which act as internal restraint and tend to hinder the free deformation, as showed by comparison between the results obtained on UHPFRC mixtures with and without fibres. The reduction of autogenous shrinkage was about 35% in presence of fibres [1], this findings is in agreement with results reported in the literature.

Figure 3 shows also that the increase of temperature increases the autogenous shrinkage. For instance, an increase of about 5% for 30°C and 32% for 40°C was obtained in comparison to mean shrinkage at 20°C, all obtained at 65 days. After 7 days, 49% of the mean value obtained at 65 days for a 30°C cure is reached, and 66% of the mean value at 65 days for a 40°C cure is reached. In fact, the evolution of autogenous shrinkage strongly slows down beyond 28 days for specimens cured at 30 and 40°C mainly due to the stabilization of hydration, as

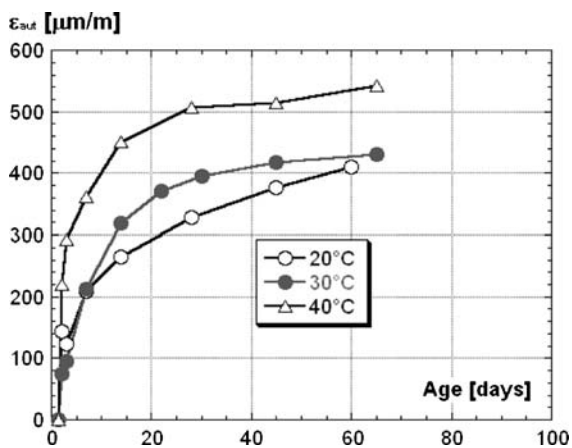


**Fig. 3** Autogenous shrinkage under different curing conditions

illustrated in Fig. 2a. The influence of temperature on the autogenous shrinkage evolution was related to the hydration and the self-desiccation processes that accelerate at higher temperatures, as shown in Fig. 2. These results are in agreement with results found in the literature [4, 5, 18].

The extrapolation of autogenous shrinkage data under the different curing conditions using an exponential model (not reported in this paper) has shown a similar trend at long term i.e. an inverse effect of temperature on the autogenous shrinkage, its amplitude is higher at 20°C when compared to that predicted at high curing temperature 30 and 40°C [1, 13].

## 5 Effect of temperature on compressive strength

The evolution of compressive strength, in the same temperature range is represented in Fig. 4. There is a clear similarity between the degree of hydration and the compressive strength curves (Figs. 2a, 4). This can be expected as the hydration contributes to the strength development in addition to other micro-structural factors. The chemical reactions of binders develop simultaneously and in an interdependent way, leading to a progressive solid skeleton formation that contributes in strength development, as well as the rearrangement of hydration products.

The inverse effect of temperature on compressive strength was also observed and takes place at

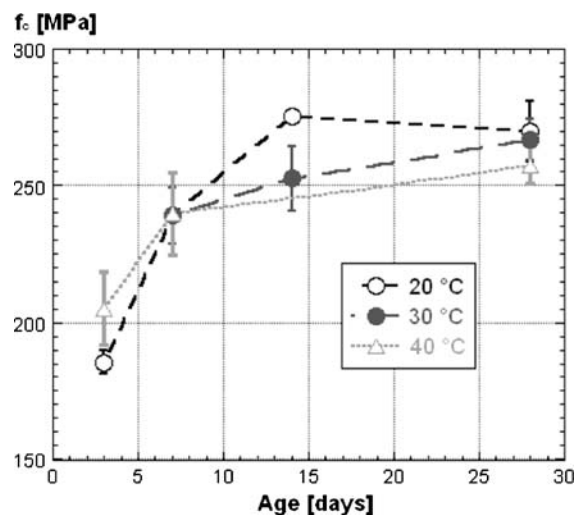


**Fig. 4** Evolution of the compressive strength for different curing conditions

approximately 7 days. This inverse effect can be explained by the same arguments given for the degree of hydration and cited in the previous section.

## 6 Prediction of UHPFRC compressive strength under different curing temperatures

### 6.1 Model description

The hyperbolic relationship (Eq. 1) was used to describe the compressive strength evolution for the considered curing temperatures in this study [2, 19]. This model describes the evolution of the compressive strength and supposes that the strength development starts after  $t_0$ . The model is based on the following equation:

$$S = \frac{S_{\infty} \cdot k(t - t_0)}{1 + k(t - t_0)} \quad (1)$$

with:  $t_0$ : the initial time of strength development,  $k$ : specific rate of reaction and  $S_{\infty}$ : ultimate strength.  $k$  and  $S_{\infty}$  are obtained by a minimization process (least square fit).

### 6.2 Predicted UHPFRC compressive strength

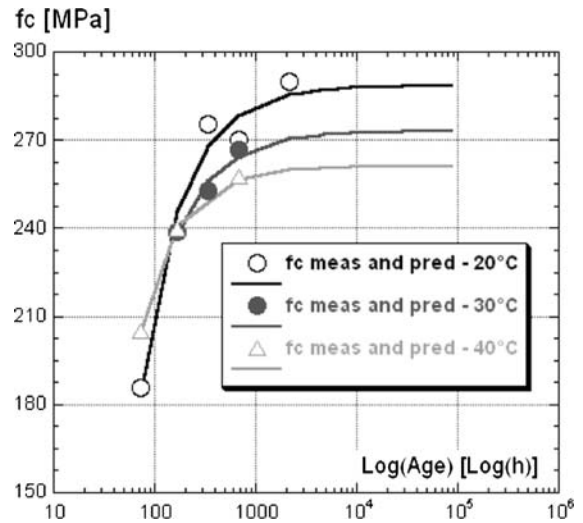
The application of this model to our experimental results under various temperatures gives the results represented in Fig. 5. The set of parameters determined for the tested UHPFRC are given in Table 5.

Figure 5 shows that the empirical model describes well the evolution of the UHPFRC compressive strength under the tested curing conditions. And the model reflects the inverse effect of the curing conditions that takes place approximately after 7 days. In fact, the predicted ultimate strength for higher temperatures 30 and 40°C are weaker than that predicted for 20°C, the reduction is of 6% and 10% respectively.

## 7 Activation energy

### 7.1 Activation energy as given in literature

In the literature, there are contradictory recommendations regarding the choice of the activation energy.



**Fig. 5** Prediction of compressive strength for different curing conditions

**Table 5** Parameters model for different curing conditions

Curing	20°C	30°C	40°C
$S_{\infty}$ (MPa)	288	273	261
$k$ (1/h)	0.04	0.05	0.09

A set of equations for the activation energy that allows representing several types of Danish cements was proposed by Hansen and Pedersen [3]:

$$\begin{aligned} \text{for } \rightarrow T \geq 20^{\circ}\text{C} &\Rightarrow E(T) = 33.5 \text{ kJ/mol} \\ \text{for } \rightarrow T < 20^{\circ}\text{C} &\Rightarrow E(T) = 33.5 + 1.470(20 - T) \\ &\text{kJ/mol} \end{aligned} \quad (2)$$

Formulation proposed by Hansen and Pedersen [3] was recommended by Rilem [20] but independently of cement type. However a high value (48.8 kJ/mol) is recommended for the cement containing blast furnace slag. In several cases, the equation proposed by Hansen and Pedersen [3] is used independently of cement and addition type.

On the other hand, according to [21], the activation energy depends on the cement chemical composition, the fineness, the type, the quantity of the cement and the used mineral addition. Other authors indicated that the activation energy varies according to the water to cement ratio. However, it was shown that the water to cement ratio has no significant effect on the activation energy [22].

Another equation to estimate the activation energy for Swedish cements at 20°C was proposed by Jonasson et al. [22]. Their equation gives an activation energy superior of 32% to that proposed by Hansen and Pedersen [3] and gives higher values for high temperatures.

Several values of the activation energy obtained (between 41 and 67 kJ/mol) are summarized by Carino and Molhotra [21], these values vary with the type of cement. However, contrary to [3], all the values of activation energy are constant and independent of the temperature. This is in agreement with the law of Arrhenius.

A constant value of activation energy (between 40 and 45 kJ/mol) is recommended by ASTM C 1074 [23] to predict the mechanical strength in situ when the cement of type I is used without additions and no indication was given for other cements and additions [24] recommended an activation energy that is a function of the hydration temperature and the development of the relative strengths. Recently, a new formulation of the activation energy dependant on temperature and degree of hydration was also proposed by Pane and Hansen [25]. A model to estimate the activation energy that considers the type of cement with and without additions (fly ash and blast furnace slag) was proposed by Schindler [26].

According to what precedes, it is evident that there are several contradictions about the choice of an appropriate value of the activation energy. And as no value of activation energy was found in literature, because investigations accounting for the thermal effect on this specific material are inexistent, we have exploited the values of the specific rate of reaction ( $k$ ) determined from the prediction of the UHPFRC compressive strength under different curing conditions (see Table 5) to evaluate the activation energy of the tested UHPFRC.

## 7.2 Estimation of activation energy of the tested UHPFRC

The variation of the specific rate of reaction ( $k$ ) can be described by the Arrhenius law [2, 19, 26, 27].

$$k = A \cdot \exp \left[ \frac{-E_a}{R \cdot T} \right] \quad (3)$$

with:  $A$ : parameter that is independent or varies slightly with temperature (1/h),  $E_a$ : activation energy

(J/mol),  $R$ : universal gas constant (8.314 J/mol/K),  $T$ : absolute temperature (K) and  $k$ : specific rate of reaction (1/h).

According to Eq. 3 the relationship between  $\ln(k)$  and the inverse of absolute temperature is linear:

$$\ln(k) = \frac{-E_a}{R \cdot T} + \ln(A) \quad (4)$$

Consequently, the value of the activation energy can be calculated from the slope of the linear plot of  $\ln(k)$  against  $(1/T)$ , as represented in Fig. 6.

The calculated value of activation energy for the tested UHPFRC is equal to 33 kJ/mol and is similar to that obtained for conventional concretes. The obtained value corresponds to the value prescribed by Hansen and Pedersen [3] and Rilem [20], and is in the range proposed by Guo [28]. The similarity between UHPFRC and normal concrete activation energies can be attributed to: (1) the low water to cement ratio in the UHPFRC, which does not influence the activation energy, contrary to what was observed by Carino and Tank [29], and (2) the presence of a high amount of silica fume (26%) which acts as fly ash on the activation energy [30]. According to the authors, the hydration in the presence of a high amount of silica fume is controlled by diffusion and the reactions controlled by diffusion lead to values of activation energy lower than the reactions controlled in interfaces [30].

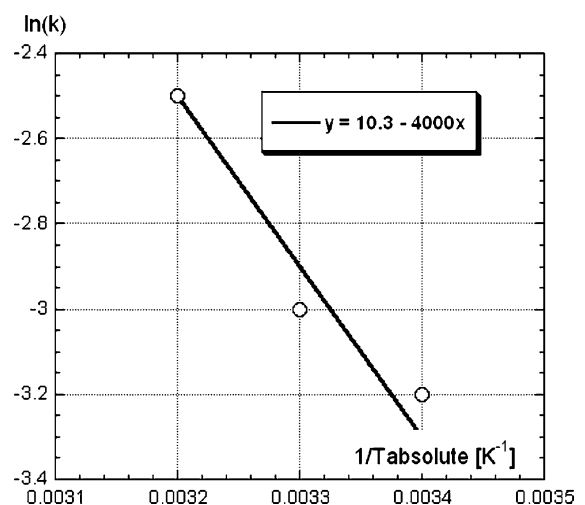


Fig. 6 Evolution of  $\ln(k)$  as function of the inverse of absolute temperature



The application of the model proposed by Schindler [26] gives a low activation energy (31.6 kJ/mol), the reduction is about 6.5% with respect to the value obtained using the current empirical model. The predicted activation energy for the current UHPFRC is used in the following section to describe the effect of temperature on autogenous shrinkage by means of the maturity concept.

## 8 Application of the maturity concept

In this part, the aim is to verify the validity of the maturity concept to predict the UHPFRC autogenous shrinkage for the studied temperatures (between 20 and 40°C).

The maturity function based on the Arrhenius law proposed by Hansen and Pedersen [3] was used to calculate the equivalent age. The equivalent age converts the chronological age ( $t$ ) of a specimen cured at any temperature  $T(t)$  to an equivalent age ( $t_{\text{equ}}$ ) cured at a specific reference temperature ( $T_{\text{ref}}$ ). The equivalent age is expressed by the following relation:

$$t_{\text{equi}} = \int_0^t \exp \left[ \frac{E_a}{R} \left( \frac{1}{273 + T_{\text{ref}}} - \frac{1}{273 + T(t)} \right) \right] dt \quad (5)$$

with:  $E_a$ : activation energy (J/mol),  $R$ : universal gas constant (8.314 J/mol/K),  $T(t)$ : actual temperature,  $T_{\text{ref}}$ : reference temperature.

The autogenous shrinkage was represented as a function of the equivalent age calculated according to the equation above, with a single value of activation energy equal to 33 kJ/mol.

Figure 7 shows that the autogenous shrinkage can be correctly predicted for 30°C beyond 14 days. On the other hand, in the case of 40°C, the concept does not describe autogenous shrinkage because the autogenous shrinkage evolution function of equivalent age is different from that for 20°C. These results are in agreement with results obtained for cement pastes at temperatures between 20 and 40°C [7].

It has been also shown in previous research works that the traditional maturity concept is not valid [4, 5, 8, 18].

According to [4], the pouzzolanic reactions have generally different activation energy from the

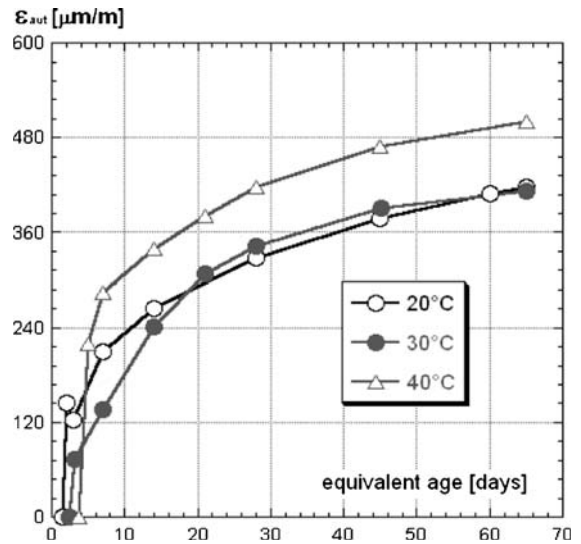


Fig. 7 Autogenous shrinkage as function of equivalent age

hydration of the cement. This indicates that the development of the properties of the concrete with additive is probably controlled by multiple activation energies. The authors of this paper agree with this argument and concluded that the single activation energy predicted by this technique can not describe all the material properties, especially the autogenous shrinkage, characterized also by an inverse effect at early age under low temperatures that can not be describe using this single activation energy [1]. However, this single activation energy describes well the heat of hydration as shown in reference [1].

In agreement with what precedes and according to [31], in theory the concrete properties that result from the combination of processes with different activation energies cannot be described by single activation energy. Despite this, in practice, the properties of concretes with additions are modelled by single activation energy. This can be acceptable as long as the property is governed by the hydration of the cement. However, the autogenous deformations, in some cases, are strongly influenced by the presence of silica fume. In that case, not only single activation energy allows a complete description of the autogenous deformation in a satisfactory way. This was validated by Jensen and Hansen [4], the authors showed that the traditional maturity concept does not apply for both autogenous shrinkage and internal relative humidity.

## 9 Conclusions

- The effect of the thermal curing on all the physico-mechanical properties studied is favourable at early age because the various processes that interact are thermo-activated at early age. However, an inverse effect was observed in the long term. This effect is attributed to the lower ultimate degrees of hydration for higher temperatures with regard to 20°C.
- The estimated activation energy for the tested UHPFRC is equal to 33 kJ/mol and is similar to that obtained for conventional concretes. This was attributed to the low water to cement ratio in the UHPFRC, which does not influence the activation energy. Finally, we can conclude that the activation energies (E) found here is correct at least for tested composition. This value must be validated by further experiments. There is, therefore, more work to be made in this field, because it is necessary to characterize and predict correctly the early age behaviour of this specific cementitious material, which is determining parameter in the structural response.
- The maturity concept is valid and describes successfully the autogenous shrinkage for temperatures between 20 and 30°C. For low and high temperatures, more work is needed in this field, in our opinion. Note finally that certain authors considered two activation energies which was validated for other cementitious materials.

**Acknowledgments** This project was financially supported by the Swiss National Science Foundation and by the Swiss Federal Office for Education and Science in the context of the European project “Sustainable and Advanced Materials for Road Infrastructures” (SAMARIS).

## References

1. Kamen A (2007a) Comportement au jeune âge et différé d'un béton écrouissant sous les effets thermomécaniques. Doctoral thesis, The Ecole Polytechnique Fédérale de Lausanne, Suisse, No. 3827, 246 pp (in French)
2. Carino NJ, Lew HS (2001) The maturity method: from theory to application. In: Chang PC (ed) Proceedings of the structures congress and exposition, May 21–23, Washington, DC. American Society of Civil Engineers, Reston, Virginia, 19 pp
3. Hansen PF, Pedersen EJ (1977) Maturity Computer for controlled curing and hardening of concrete. *Nord Betong* 1(19):21–25
4. Jensen OM, Hansen PF (1999) Influence of temperature on autogenous deformation and relative humidity change in hardening cement paste. *Cement Concr Res* 29:567–575. doi:10.1016/S0008-8846(99)00021-6
5. Bjontegaard O (1999) Thermal dilatation and autogenous deformation as driving forces to self-induced stresses in high performance concrete. Doctoral thesis, The University of Trondheim, Norway, 256 pp
6. Loukili A, Chopin D, Khelidj A, Le Touzo J-Y (2000) A new approach to determine autogenous shrinkage of mortar at an early age considering temperature history. *Cement Concr Res* 30:915–922. doi:10.1016/S0008-8846(00)00241-6
7. Turcry P, Loukili A, Casabonne JM (2002) Can the maturity concept be used to separate the autogenous shrinkage and thermal deformation of a cement paste at early age. *Cement Concr Res* 32:1143–1450. doi:10.1016/S0008-8846(02)00800-1
8. Mounouga P (2004) Etude expérimentale du comportement de pâtes de ciment au très jeune âge: hydratation, retraits, propriétés thermophysiques. Doctoral thesis, The University of Nantes, France, 217 pp (in French)
9. Rossi P, Arca A, Parant E, Fakhri P (2005) Bending and compressive behaviours of a new cement composite. *Cement Concr Res* 33:27–33. doi:10.1016/j.cemconres.2004.05.043
10. Habel K (2004) Structural behaviour of elements combining ultra-high performance fibre-reinforced concretes (UHPFRC) and concrete. Doctoral thesis, The Ecole Polytechnique Fédérale de Lausanne, Suisse, No. 3036, 195 pp
11. Kamen A, Denarié E, Brühwiler E (2006) Physico mechanical properties of ultra high performances fibre reinforced concrete. In: Proceedings of the first mediterranean symposium in advances on geomaterial and structures. Hammamet, Tunisia, 3–5 May, pp 643–648
12. Kamen A, Denarié E, Brühwiler E (2005) Mechanical behavior of ultra high performance fiber reinforced concretes (UHPFRC) at early age, and under restraint. In: Pijaudier-Cabot G, Gérard B, Acker P (eds) Proceedings of the CONCREEP 7, September 12–14, 2005, Nantes, France. Hermès Publishing, pp 591–596
13. Kamen A (2006) Time dependent behaviour of ultra high performance fibre reinforced concrete. In: Proceedings of the 6th international PhD symposium in civil engineering, Zurich, August 23–26 (book with extended summaries and CD-ROM with full papers)
14. Verbeck GJ, Helmuth RH (1969) Structure and physical properties of cement paste. In: Proceedings of the 5th international congress on the chemistry of cement, Tokyo, Japan, pp 1–32
15. Kjellsen KO, Detwiler RJ, Gjorv OE (1991) Development of microstructures in plain cement pastes hydrated at different temperatures. *Cement Concr Res* 21:179–189. doi:10.1016/0008-8846(91)90044-1
16. Kjellsen KO, Detwiler RJ (1992) Reaction kinetics of portland cement mortars hydrated at different temperatures. *Cement Concr Res* 22:112–120. doi:10.1016/0008-8846(92)90141-H
17. Kamen A, Denarié E, Brühwiler E (2007) Thermal effects on physico-mechanical properties of UHPFRC. *ACI Mater J* 104(4):415–423



18. Charron J-P (2003) Contribution à l'étude du comportement au jeune âge des matériaux cimentaires en conditions des déformations libre et restreinte. Doctoral thesis, The University of Laval, Québec, Canada, 332 pp (in French)
19. Barnett SJ, Soutsos MN, Millard SG, Bungey JH (2006) Strength development of mortars containing ground granulated blast-furnace slag: Effect of curing temperature and determination of apparent activation energies. *Cement Concr Res* 36:434–440. doi:[10.1016/j.cemconres.2005.11.002](https://doi.org/10.1016/j.cemconres.2005.11.002)
20. Rilem TC 119-TCE (1997) Avoidance of thermal cracking in concrete at early ages. *Materials and Structures RILEM*, 30:451–464
21. Carino JN, Molhotra VM (1991) Maturity method. In: Molhotra VM, Carino JN (eds) *CRC handbook on non-destructive testing of concrete*. CRC Press, pp 101–146
22. Jonasson JE, Groth P, Hedlund H (1995) Modeling of temperature and moisture field in concrete to study early age movements as a basis for stress analysis. In: *Proceedings of the int. RILEM symp. on thermal cracking in concrete at early age*, E & FN SPON, London, pp 45–52
23. ASTM C 1074 (1998) Standard practice for estimating concrete strength by the maturity method. ASTM C 1074 International, West Conshohocken (cited by Schindler AK (2004) *ACI Mater J* 101(9):72–80)
24. Kjellsen KO, Detwiler RJ (1993) Later-age strength prediction by a modified maturity model. *ACI Mater J* 90:220–226
25. Pane I, Hansen W (2002) Concrete hydration and mechanical properties under nonisothermal conditions. *ACI Mater J* 99:534–542
26. Schindler AK (2004) Effect of temperature on hydration of cementitious materials. *ACI Mater J* 101(9):72–80
27. Tank RC, Carino JN (1991) Rate constant functions for strength development of concrete. *ACI Mater J* 88(1):74–83
28. Guo C (1989) Maturity of concrete: method for predicting early stage strength. *ACI Mater J* 86:341–353
29. Carino NJ, Tank RC (1992) Maturity functions for concretes made with various cements and admixtures. *ACI Mater J* 89(2):188–196
30. Ma W, Sample D, Martin R, Brown PW (1994) Calorimetric study of cement blends containing fly ash, silica fume and slag at elevated temperatures. *Cement Concr Agg* 16(2):93–99. doi:[10.1016/0958-9465\(94\)90004-3](https://doi.org/10.1016/0958-9465(94)90004-3)
31. Korhonen U, Vilhonen E (1963) On the calculation of activation energy in thermal activation rate processes. *Acta Polytech Scand, Series Ch. N° 22*